An Investigation of Scratch Testing of Silicone Elastomer Coatings with a Thickness Gradient

James G. Kohl,[1] Nicholas X. Randall,[2] Norbert Schwarzer,[3] Truc T. Ngo,[1] J. Michael Shockley,[2] Rahul P. Nair[2]

[1]*Department of Engineering, University of San Diego, San Diego, California 92110-2492*
[2]*CSM Instruments, Needham, Massachusetts 02494*
[3]*Saxonian Institute of Surface Mechanics SIO, Am Lauchberg 2, 04838 Eilenburg, Germany*

Received 14 March 2011; accepted 23 July 2011
DOI 10.1002/app.35325
Published online 3 November 2011 in Wiley Online Library (wileyonlinelibrary.com).

ABSTRACT: Silicone elastomer coatings are currently being investigated as foul release coatings on ships hulls. Previous tests on silicone duplex elastomer coatings used a progressive load scratch test. It has been shown that the durability of uniform silicone duplex elastomer coatings is a function of thickness, indentation modulus, and stylus and that the failure mechanism depended on coating thickness and stylus. When applying silicone coatings to a ship's hull, there are regions on the ship where the coating is not uniform. This article investigates the effect of a thickness gradient on the durability of a single layer silicone elastomer coating. In these tests, a constant normal load was used as the stylus moved transversely to the surface. It was found that when the scratch test started in the silicone coating and proceeded in the direction of decreasing coating thickness ("Elastomer to Metal"), there was first a scratch tract followed by the initiation of detachment of the coating, then by gross detachment of the coating. When the scratch started on the exposed aluminum surface and proceeded into the silicone in the direction of increasing coating thickness ("Metal to Elastomer"), there was first gross detachment of the coating, followed by recovery (i.e., silicone coating is intact) and a scratch tract into the silicone. It was also found that the coefficient of friction was much higher in the silicone when the scratch test was going in the direction of decreasing coating thickness as opposed to the scratch test going in the opposite direction. © 2011 Wiley Periodicals, Inc. J Appl Polym Sci 124: 2978–2986, 2012

Key words: adhesion; coatings; elastomers; silicones; failure

INTRODUCTION

Silicone-based elastomer coatings are being investigated as foul release coatings. It has been shown that the foul release properties are dependent on the elastic modulus, work of adhesion, and coating thickness.[1–3] In assessing these coatings durability as foul release coatings, progressive load scratch testing (normal force increasing as sample slides) have been performed on coatings with uniform thicknesses.[4–6] The parameter that was used to quantify the durability[4,6] for silicone bi-layer coatings was a critical tangential force, T_c. The critical tangential force is the value of tangential force which precedes a dip in the tangential force versus normal force plot and corresponds with the onset of failure. It was shown that T_c increased as both the top coat and bond coat thickness increased such that

$$T_c = a_1 t_t + a_2 t_b \quad (1)$$

where a_1 and a_2 are constants, and t_t and t_b are the top coat thickness and bond coat thickness, respectively. It was also observed that there were two types of failure mechanisms depending on stylus geometry and bond coat thickness.[4] One failure mechanism was tearing of the top coat. This was associated with sharper stylus and thin bond coat. The other type of failure mechanism was bond coat detachment from the substrate. This was observed when a blunted stylus was used on thicker bond coats. At intermediate bond coat thickness both failure mechanisms were observed. The durability was also found to be dependent on the modulus of elasticity.[6]

When applying a coating on a ship's hull, there will most likely be regions in the coating which do not have a uniform thickness.[7] It has been shown that the release behavior is dependent on the thickness gradient of the coating.[8] It is the purpose of this study to determine the effects of the presence of a thickness gradient on the durability of a single layer silicone coating.

Of special importance for this work is the modeling of multiaxial indentation tests. There exist numerous works for the analysis and simulation of

Correspondence to: J. G. Kohl (jkohl@sandiego.edu).

these experiments, usually referred to as scratch or tribo tests.[9–17] Here, typically a diamond stylus (normally spherical diamond tip geometry) is utilized to apply a normal load, N, onto the sample surface. Simultaneously, the sample is displaced at a constant speed while the load is increased. At some point, the resulting stresses cause failure like fracture or plastic deformation, resulting in flaking, chipping at the coating–substrate interface or between the coatings finally leading to complete delamination of the coating. The tangential critical force (T_c) at which a specific failure event occurs can be recorded from the fluctuation in the tangential force, from the acoustic emission signal, or can be observed as specific surface deformation in the optical microscope. T_c can also be detected as a discontinuity (step) in the postsurface scan. It is obvious that in addition to the normal force, the indenter geometry applying that force, the surface, and the interface geometry of the coating–substrate system are variables which influence the result of the test. In previous studies, the complexity of the test initiated numerous investigations to elucidate the scratch process in more detail. Coating adhesion and aging[18] and the correlation between hardness and adhesion[19] were studied. Theoretical explanations of the scratch test based on an energy approach[20] and the interfacial surface energy and elastic constants[3] were also derived. Additionally, models of the scratch test were developed. Burnett and Rickerby[21] modeled the stresses generated during the scratch test as a combination of an indentation stress field, a frictional stress field, and the residual (internal) stress present in the coating. Based on this model, Bull et al.[22] demonstrated the importance of each of these stresses in determining the levels of adhesion for a number of titanium nitride coated substrates. Finite Element Modeling (FEM) was used in the approaches of Hegadekatte, Huber and coworkers[9–11] to simulate tribological tests, like pin on disc. Of outstanding importance and quality, however, are surely the contributions of Holmberg et al.[12–17] Here also FEM was used to investigate scratch tests, not only with respect to stresses and strains occurring during the scratch but also with respect to material deformations, the influence of coating thickness, and Young's modulus as well as the question of fracture toughness calculation and the influence of residual stresses.

Unfortunately, all these models are numerically based (FEM or Boundary Element Method) and thus can neither be inverted in an easy manner nor do they allow the necessary quick evaluation on sufficiently simple computer systems to investigate complex coating systems used in the industry as an "every day test." That is why one of the authors in the present study (Schwarzer) has developed three-dimensional general contact solutions for layered materials applicable for arbitrary normal, lateral, tilting, and twisting loads.[23,24] These models are completely analytical. As a drawback, the models are completely elastically based, but this has been compensated for by measuring and incorporating the residual indentation depth into the model. This is possible by the so called "effective indenter concept" on which also the classical Oliver and Pharr method for the analysis of nanoindentation data[25] is based. However, for layered materials and multi-axial indentation (scratch) an extension was required. This extension is due to the well established fact, that the classical Oliver and Pharr method[25] and thus its "effective indenter concept," as an approach based upon the model of a completely homogeneous half space, cannot directly be applied to layered materials and small structures [e.g., [26]]. Already in 1995[27] Pharr introduced the "Concept of the Effective Indenter" and refined it in a series of wonderful publications until in 2002 and 2004 two papers about "Understanding of nanoindentation unloading curves"[28,29] were published. In 2004, one of the present coauthors (Schwarzer) developed an approach solving not only the problem for the mechanical contact of an indenter with general shape of symmetry of revolution as theoretical basis for the "concept of the effective indenter," but also to extend this solution to layered structures.[30,31] It is beyond the scope of this article to repeat the structural basics of the model or to demonstrate its application for multiaxial contact simulations or the method of extracting true coating parameters. Thus, the reader is referred to a variety of references published together with Pharr, Bemporad, Derby, Griepentrog, Chudoba, Richter and many others.[6,32–44] Among these are:

- determination of yield strength of homogeneous materials via nanoindentation with sharp indenters[30,45]
- determination of true Young's modulus and yield strength of "standard" coating materials via nanoindentation with sharp indenters[32–37]
- determination of true Young's modulus and yield strength of coating materials of ultra thin coatings with thicknesses well below 100 nm via nanoindentation with sharp indenters[38,39]
- determination of true Young's modulus and yield strength of unusual or tricky coating materials via nanoindentation with sharp indenters[6,41–44]
- determination of true Young's modulus, yield strength, and residual stresses of coating materials via nanoindentation with sharp indenters.[23]

Finally, an extension of the analytical contact solutions to arbitrary lateral, tilting, and twisting loads

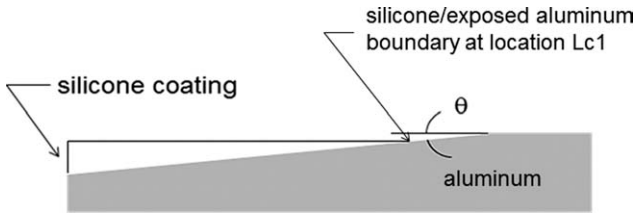

Figure 1 Schematic of silicone coating with thickness gradient on a milled aluminum block.

was developed to allow the simulation and analysis of more practical experiments like scratch and tribo tests.[24,25] For practical use, these results have been incorporated into most flexible software packages allowing quick and quite comfortable modeling,[46,47] namely FilmDoctor which has been used in the "Model of Thickness Effects on Coefficient of Friction" section of the present article.

EXPERIMENTAL METHODS

Aluminum 6061 block with the dimensions 50 mm × 75 mm × 10 mm were milled to produce the following angles: for Sample A, $\theta = 2.862°$; for Sample B, $\theta = 4.289°$; and for Sample C, $\theta = 5.711°$ (refer to Fig. 1 for definition of θ), then glass bead peened. The inclined surface was then coated with a thin layer of primer coating (Wacker® Primer G 790). A layer of masking tape was used to surround the inclined surface to serve as a bath to pour the uncured silicone (Dow Corning Corp.'s Sylgard® 184). The silicone was poured into the bath to a level at which the surface was still inclined. The silicone was then allowed to cure to form the silicone elastomer coating.

A CSM Instruments Revetest (S/N 01-2617) was used to perform the scratch testing. The aluminum substrates were attached to the steel mounting pucks using a quick drying adhesive. The pucks were in turn mounted on the Revetest using pins on a universal sample holder as shown in Figure 2. A 6-mm 100Cr6 steel ball was used as the contact stylus. A constant normal load of 20 N was applied while the stylus moved transversely across the silicone coating at a speed of 50 mm/min. The length of the scratch tract was approximately 8 mm. The data acquisition rate was 10 Hz.

Two sets of three scratch tests each were performed near where the silicone meets the exposed aluminum on each angled sample (see Fig. 1). For one set, the scratch test started in the silicone coating and proceeded in the direction of decreasing coating thickness. This set of tests will be referred to as "Elastomer to Metal" in that the scratch starts in the silicone and proceeds to the exposed aluminum surface. For the other set, three scratch tests were performed starting on the exposed aluminum surface and then proceeding into the silicone in the direction of increasing coating thickness. This set of tests will be referred to as "Metal to Elastomer."

RESULTS AND DISCUSSION

Pictures of the scratch tract and plots of the coefficient of friction (= tangential force ÷ normal force) were matched. In other words, the location along the scratch tract corresponds to the same location on the coefficient of friction plot. Typical scratch tract pictures and corresponding coefficient of friction plots for the "Elastomer to Metal" (direction of decreasing coating thickness) and "Metal to Elastomer" (direction of increasing coating thickness) are shown in Figures 3 and 4, respectively. From Figure 3, when the scratch begins in the silicone the scratch tract starts almost immediately at the beginning (location Lc4 on picture) of the test. The coefficient of friction at this location is the maximum value in the silicone coating before the initiation of detachment occurs and is designated here as μ_{max}. The scratch then proceeds until the initiation of detachment of the

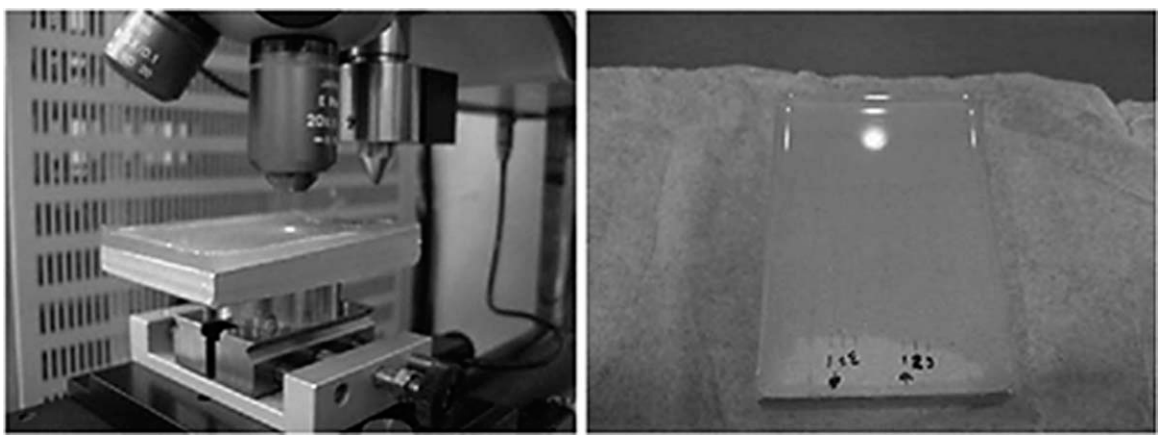

Figure 2 A sample as mounted (left); a sample after testing, showing scratch numbers and direction (right).

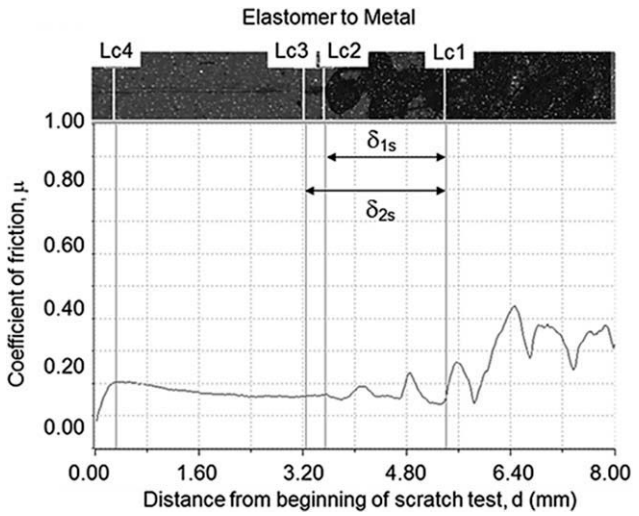

Figure 3 Typical micrograph of scratch tract and plot of the coefficient of friction for the set of scratch tests starting in the silicone coating and proceeding in the direction of decreasing coating thickness ("Elastomer to Metal" tests).

coating from the aluminum (location Lc3 on picture) or when the aluminum surface is first observed. The coefficient of friction at this location is designated as μ_{init}. This is followed by the onset of gross detachment of the coating (location Lc2 on picture), defined here as when there is large amounts of silicone removed from the surface. Location Lc1 in both figures represent the silicone/exposed aluminum boundary and serves as the common reference location. From Figure 4, when the scratch begins at the silicone/exposed aluminum boundary (Lc1), gross detachment of the coating occurs immediately and ends at Lc2. As the stylus proceeds into the silicone, there is a point where the silicone remains intact and adhered to the aluminum. This point is referred to here as complete recovery and occurs at Lc3. The coefficient of friction at this location is μ_{rec}. As the stylus proceeds further, it forms a scratch tract in the silicone that is still intact. Lc4 in this figure corresponds to the same location as to where the maximum coefficient of friction of the intact silicone coating occurred in the "Elastomer to Metal" scratch test (Lc4 in Fig. 3). The coefficient of friction at Lc4 in Figure 4 is referred to as μ_{corr}. Since μ_{corr} is measured at the same distance from Lc1 as μ_{max} is in the corresponding "Elastomer to Metal" scratch test, these values of coefficient of friction may then be compared to each other.

Another observation from Figures 3 and 4 is that coefficient of friction decreases as the silicone coating thickness decreases. This friction dependence on coating thickness is consistent with previous studies performed on coatings with uniform thickness[4,6] and was true whether the scratch test direction was in the direction of increasing thickness ("Metal to Elastomer") or in the direction of decreasing thickness ("Elastomer to Metal").

Scratch tracts for Samples A, B, and C for the "Elastomer to Metal" scratch tests and for the "Metal to Elastomer" scratch tests, are shown in Figures 5 and 6, respectively. A comparison bar chart of μ_{max} and μ_{corr} is shown in Figure 7. These values are compared with each other because both of these values occur at the same location with respect to Lc1. A comparison bar chart of μ_{init} and μ_{rec} is shown in Figure 8. From these two figures it can be seen that the coefficient of friction is much greater ($\mu_{max}/\mu_{corr} \sim 2.6$–$3.4$ at location Lc4) for the case when the stylus proceeds in the direction of decreasing coating thickness ("Elastomer to Metal"). For the scratch tests performed in this direction ("Elastomer to Metal"), the presence of an inclined interface results in the stylus trying to horizontally compress the silicone toward the much harder aluminum. For the scratch tests performed in the direction of increasing coating thickness ("Metal to Elastomer"), the stylus is horizontally compressing only against the silicone. It is also observed for each set of tests that the coefficient of friction decreases as the coating thickness decreases, as seen in Figures 3 and 4. However, this thickness dependence is relatively minor when compared to the inclined interface effect.

The distance between the silicone/exposed aluminum boundary (Lc1) and the start of gross detachment (Lc2) is defined as δ_{1s} (refer to Fig. 3) for the "Elastomer to Metal" tests. The distance between the silicone/exposed aluminum boundary (Lc1) and the end of gross detachment (Lc2) is defined as δ_{1e}

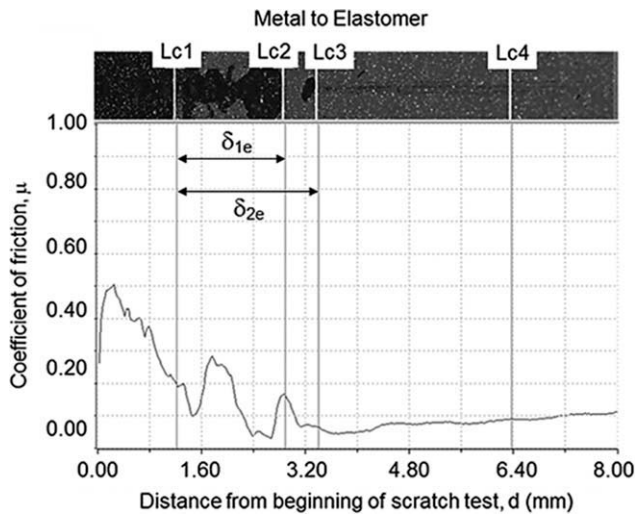

Figure 4 Typical micrograph of scratch tract and plot of the coefficient of friction for the set of scratch tests starting on the exposed aluminum surface and then proceeding into the silicone in the direction of increasing coating thickness ("Metal to Elastomer" tests).

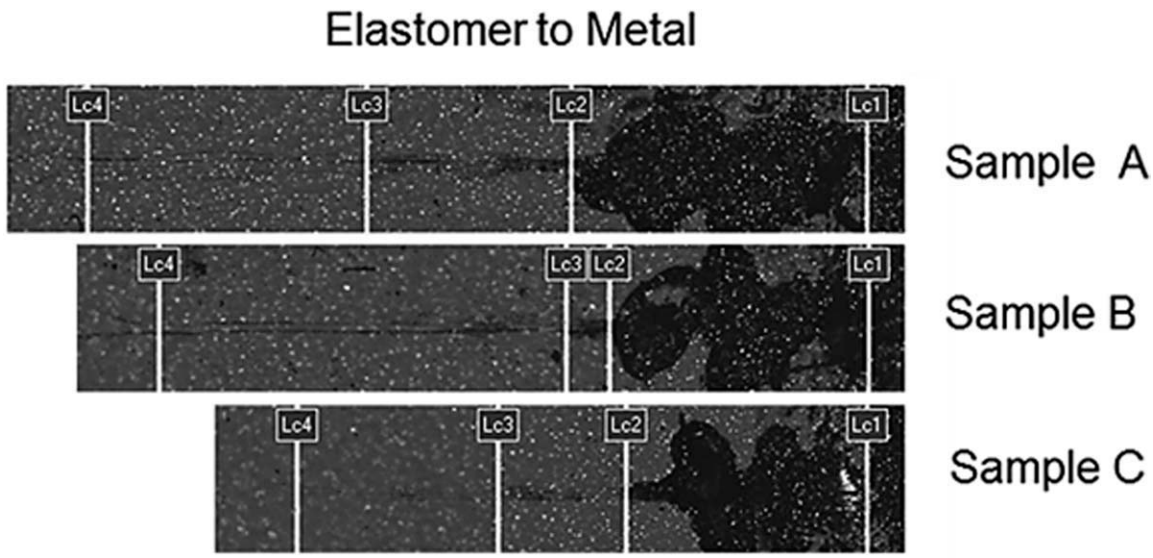

Figure 5 Micrographs of the scratch tract for the "Elastomer to Metal" direction showing the silicone/exposed aluminum boundary, Lc1; beginning of gross detachment of the coating, Lc2; initiation of detachment of the coating, Lc3; and the location of maximum coefficient of friction in the intact silicone coating (between the beginning of the test and Lc3), Lc4 (Sample A, $\theta = 2.862°$; Sample B, $\theta = 4.289°$; Sample C, $\theta = 5.711°$).

(refer to Fig. 4), for the "Metal to Elastomer" tests. A comparison chart of these two distances is shown in Figure 9. From this chart it can be seen that recovery from gross detachment happens farther away from the silicone/exposed aluminum boundary than where gross detachment begins in the silicone. In other words, recovery occurs at higher thickness values than the initiation of the gross detachment when tested in the opposite direction. It was also seen that the distance between the silicone/exposed aluminum boundary and the initiation of detachment, δ_{2s} (refer to Fig. 3), for the "Elastomer to Metal" tests was less than the distance between silicone/exposed aluminum boundary and the total recovery from detachment, δ_{2e} (refer to Fig. 4), for the "Metal to Elastomer" tests as shown in Figure 10. A possible explanation for this behavior is that for the "Metal to Elastomer" tests, the gross detachment occurred at the start of the tests and therefore subsequent detachment can occur more readily. In the other case for "Elastomer to Metal" tests, the detachment has to first initiate before gross detachment occurs.

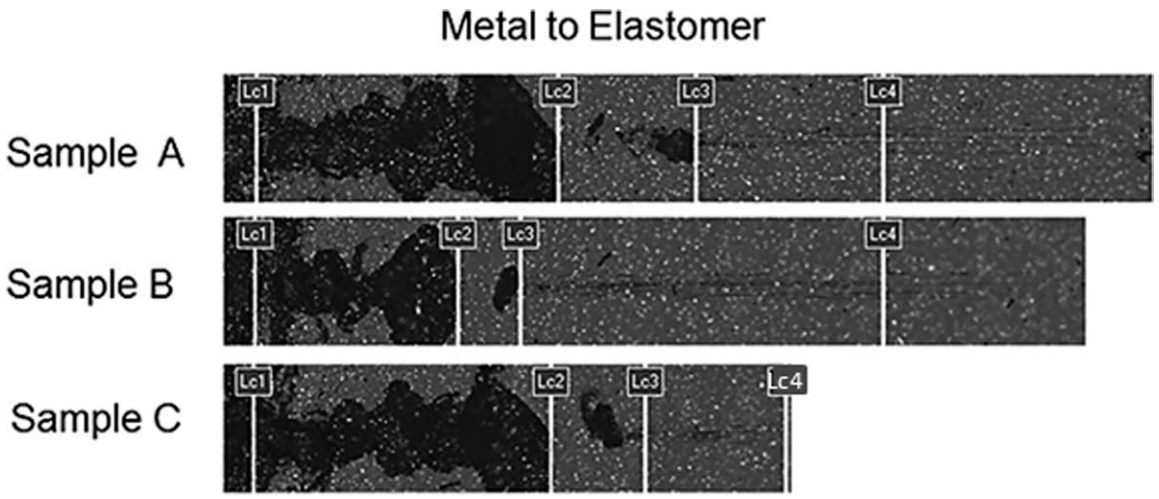

Figure 6 Micrographs of the scratch tract for the "Metal to Elastomer" direction showing the silicone/exposed aluminum boundary, Lc1; end of gross detachment of the coating, Lc2; full recovery, Lc3; and the location referenced from the elastomer/metal boundary corresponding to the location of maximum coefficient of friction in the intact silicone coating for scratches in the "Elastomer to Metal" direction, Lc4 (Sample A, $\theta = 2.862°$; Sample B, $\theta = 4.289°$; Sample C, $\theta = 5.711°$).

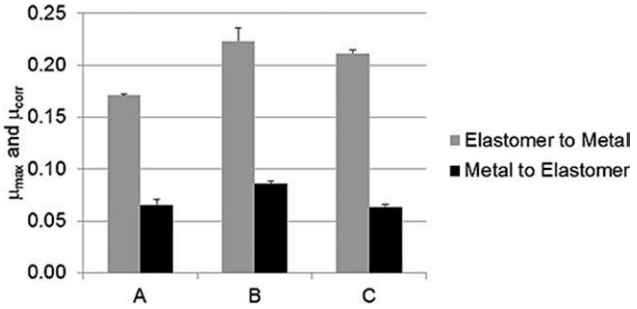

Figure 7 Maximum coefficient of friction in elastomer, μ_{max}, for the "Elastomer to Metal" tests and the coefficient of friction, μ_{corr}, at the corresponding location of μ_{max} in the silicone for the "Metal to Elastomer" tests (Sample A, $\theta = 2.862°$; Sample B, $\theta = 4.289°$; Sample C, $\theta = 5.711°$).

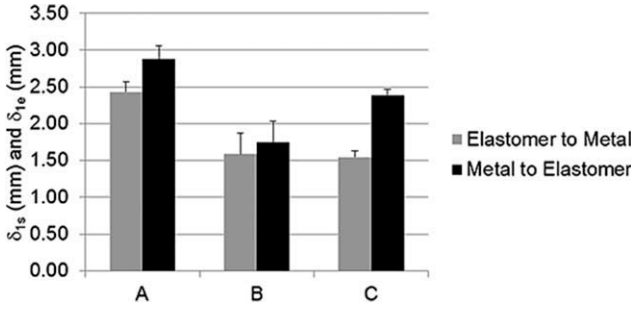

Figure 9 Distance from silicone/exposed aluminum boundary to the start of gross detachment, δ_{1s}, for the "Elastomer to Metal" tests and the distance from silicone/exposed aluminum boundary to the end of gross detachment, δ_{1e}, for the "Metal to Elastomer" tests (Sample A, $\theta = 2.862°$; Sample B, $\theta = 4.289°$; Sample C, $\theta = 5.711°$).

Model of thickness effects on coefficient of friction

Using FilmDoctor,[46] an indentation analysis was performed to explain the thickness dependence on the coefficient of friction. The resulting displacement field and von Mises stress distribution for 1 mm thick silicone (Sylgard 184—modulus of elasticity, $E = 4$ MPa,[3] and Poisson's ratio, $\nu = 0.5$) elastomer coating on an aluminum substrate (the indenter is 6 mm steel ball, the assumed "local" friction coefficient is 0.1, indentation load is 20 N) was evaluated with the results shown in Figure 11. Next, using the same indentation load, the same analysis was performed on a 3 mm thick silicone (Sylgard 184) elastomer coating with the results shown in Figure 12. As can be seen from Figures 11 and 12, the indenter on the thicker coating settles much deeper into the material and thus has to climb a steeper and higher wall. This explains the higher measured "effective" friction coefficient for thicker coatings. It should be pointed out here, that the effective friction coefficient has nothing to do with the true local friction coefficient between the surfaces of indenter and sample, but is simply the quotient of measured lateral load and normal load.

The next effect to discuss is the high difference between the effective fiction coefficients when the indenter moves from the silicone towards the exposed aluminum and from the exposed aluminum to the silicone. For this a contact solution with inclined or curved interfaces would be required. Such a solution can in principle be derived by the means of the method of the "hypothetically anisotropic space" in properly chosen curvilinear coordinates.[48] However, as the development of such an apparatus is beyond the scope of this article and we therefore refer to a simpler method.

In principle, the contact region could also be modeled by an array of load-dots as shown in the Figure 13. With such an array placed on a structure with an inclined interface with decreasing thickness in positive x-direction the displacement of the load dots for $x > 0$ would be smaller than for those with $x < 0$ (as was just proved with the aid of Figs. 11 and 12). This, however, immediately results in an inclined contact situation (as shown in Fig. 14) which automatically produces an additional downhill slope force in direction of $-x$ adding up to the

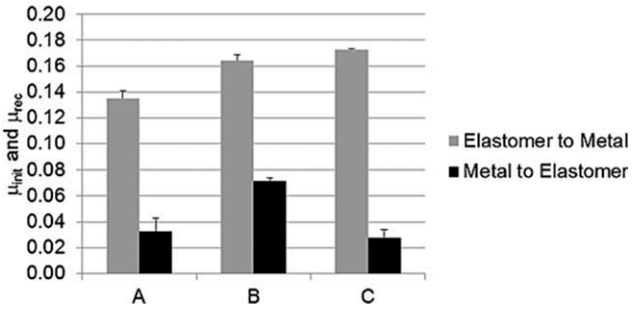

Figure 8 Coefficient of friction at initiation of detachment of the silicone coating for the "Elastomer to Metal" tests, μ_{init} and the coefficient of friction at full recovery in the silicone coating for the "Metal to Elastomer" tests, μ_{rec} (Sample A, $\theta = 2.862°$; Sample B, $\theta = 4.289°$; Sample C, $\theta = 5.711°$).

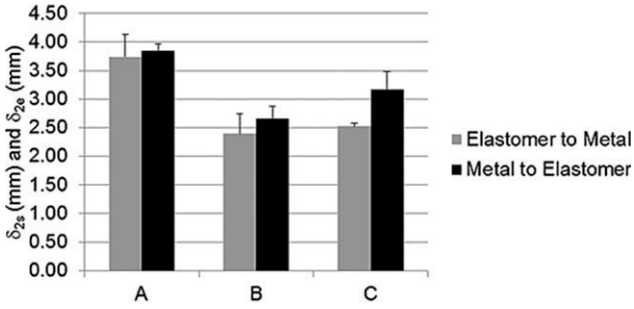

Figure 10 Distance from silicone/exposed aluminum boundary to initiation of detachment, δ_{2s}, for the "Elastomer to Metal" tests and recovery from detachment, δ_{2e}, for the "Metal to Elastomer" tests (Sample A, $\theta = 2.862°$; Sample B, $\theta = 4.289°$; Sample C, $\theta = 5.711°$).

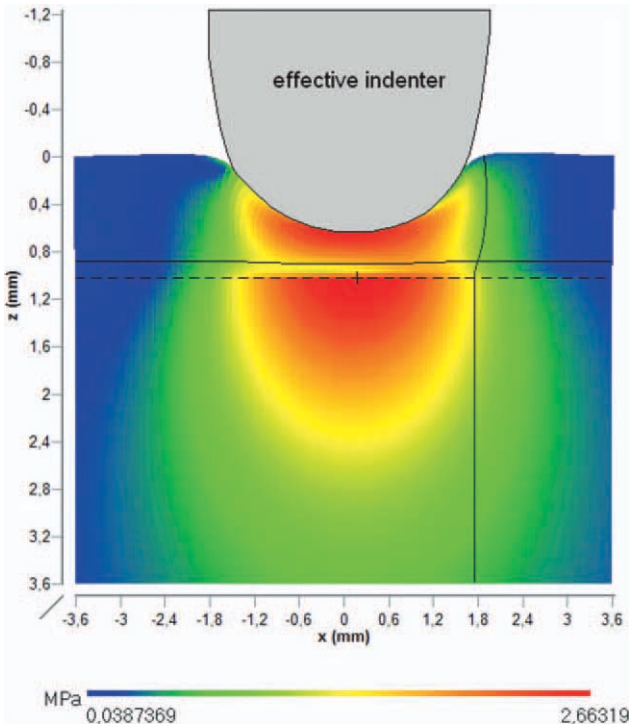

Figure 11 Displacement field and von Mises stress distribution for an indentation load of 20 N on a 1 mm thick silicone (Sylgard 184) elastomer coating on an aluminum substrate. [Color figure can be viewed in the online issue, which is available at wileyonlinelibrary.com.]

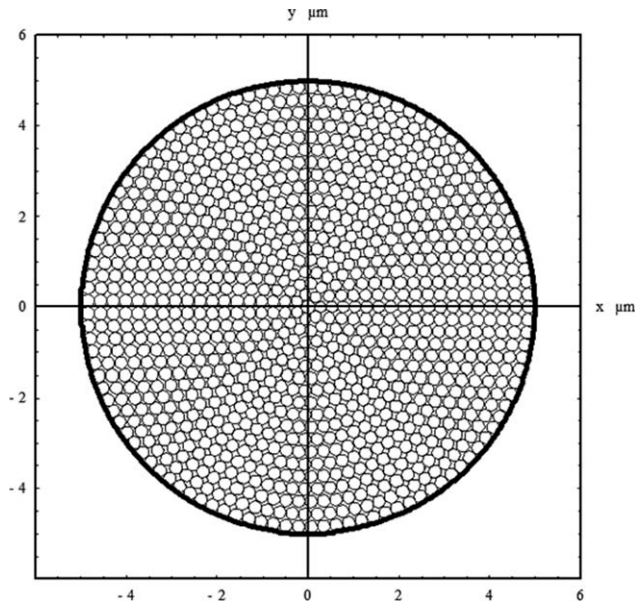

Figure 13 Example of a circular array of load dots.

lateral resistance being measured as lateral load and then given out again as "effective" friction coefficient.

If now the indenter is dragged in direction of $+x$ (decreasing thickness of silicone) the lateral

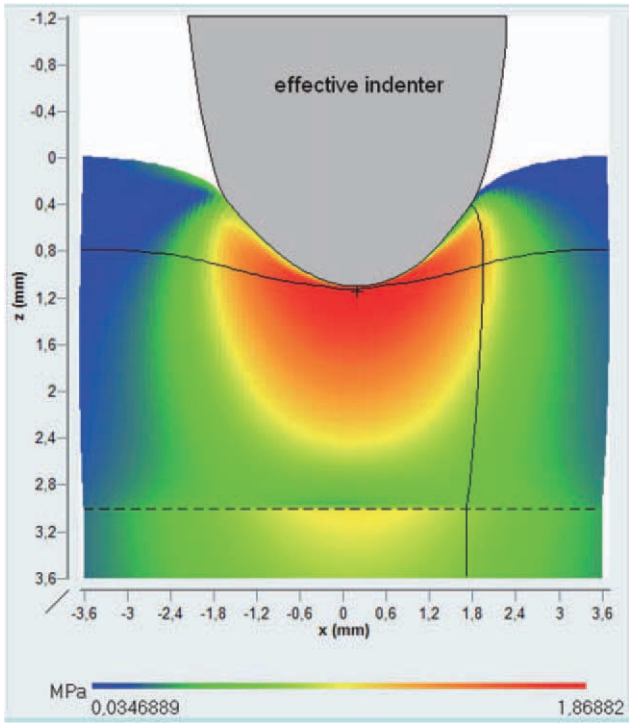

Figure 12 Displacement field and von Mises stress distribution for an indentation load of 20 N on a 3 mm thick silicone (Sylgard 184) elastomer coating on an aluminum substrate. [Color figure can be viewed in the online issue, which is available at wileyonlinelibrary.com.]

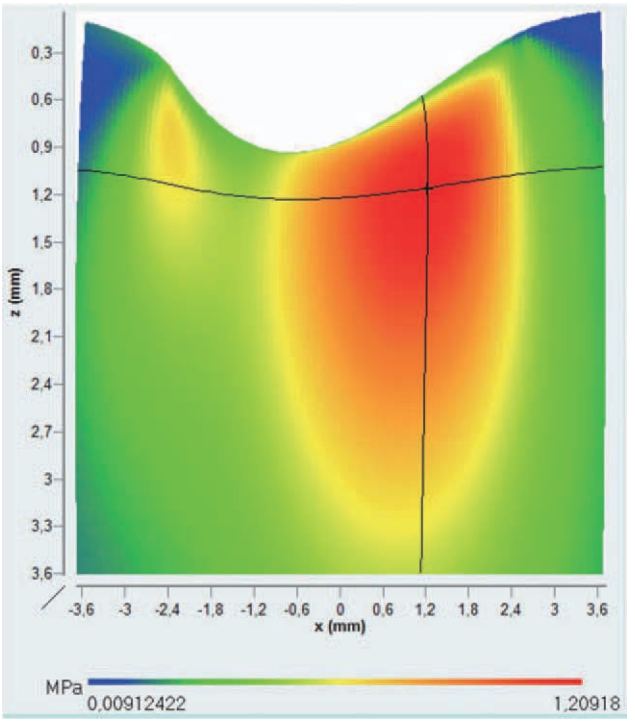

Figure 14 Displacement field and von Mises stress distribution for an indentation load of 20 N on silicone (Sylgard 184) elastomer coating on an aluminum substrate with an inclined angle of $\theta = 5.711°$.[Color figure can be viewed in the online issue, which is available at wileyonlinelibrary.com.]

resistance increases because the down-hill slope force acts against the moving direction of the indenter.

If the indenter is dragged in direction of $-x$ (increasing thickness of silicone) the lateral resistance decreases because the down-hill slope force acts in the moving direction of the indenter.

SUMMARY

It was found that when the scratch test started in the silicone coating and proceeded in the direction of decreasing coating thickness ("Elastomer to Metal"), there was first a scratch tract followed by the initiation of detachment of the coating from the aluminum, then by gross detachment. When the scratch started on the exposed aluminum surface and proceeded into the silicone in the direction of increasing coating thickness ("Metal to Elastomer"), there was first gross detachment, followed by recovery (i.e., silicone coating is intact) and then a scratch tract in the silicone.

It was observed that for the "Metal to Elastomer" tests, recovery from gross detachment happens farther away from the silicone/exposed aluminum boundary than where gross detachment begins in the "Elastomer to Metal" tests. The distance between the silicone/exposed aluminum boundary and the initiation of detachment for the "Elastomer to Metal" tests was also less than the distance between silicone/exposed aluminum boundary and the total recovery of detachment for the "Metal to Elastomer" tests. For both of these comparisons, recovery happens at higher thickness values than initiation. For elastomer foul release coatings with regions containing a thickness gradient, this means that if a detachment of the coating occurs in the thin section it may recover as the coating thickness increases thereby limiting the amount of damage.

It was also found that the coefficient of friction was much higher in the silicone when the scratch test was going in the direction of decreasing coating thickness as opposed to the scratch test going in the opposite direction. This was probably due to the inclined interface effect between the silicone and the aluminum in that the stylus is horizontally compressing the silicone into the aluminum when the scratch test direction is the same as decreasing coating thickness. It was also observed that the coefficient of friction in the silicone also increased as the coating thickness increased.

References

1. Kohl, J. G.; Singer, I. L. Prog Org Coat 1999, 36, 15.
2. Singer, I. L.; Kohl, J. G.; Patterson, M. Biofouling 2000, 16, 301.
3. Kendall, K. J Phys D Appl Phys 1971, 4, 1186.
4. Kohl, J. G.; Singer, I. L.; Griffith, J. R. Rubber Chem Technol 2000, 73, 607.
5. Zhang, S. L.; Tsou, A. H.; Li, J. C. M. J Polym Sci Part B: Polym Phys 2002, 40, 1530.
6. Kohl, J. G.; Singer, I. L.; Schwarzer, N.; Yu, V. Y. Prog Org Coat 2006, 56, 220.
7. Ingle, M.; with Naval Sea Systems Command, Private communication, 2006.
8. Kohl, J. G.; Burke, A. J; Landas, E. L. L.; Jacobitz, F. G. Prog Org Coat 2007, 59, 278.
9. Hegadekatte, V.; Huber, N.; Kraft, O. Model Simul Mater Sci Eng 2005, 13, 57.
10. Hegadekatte, V.; Huber, N.; Kraft, O. Tribol Lett 2006, 24, 51.
11. Steiner, L.; Bouvier, V.; May, U.; Hegadekatte, V.; Huber, N. Wear 2010, 268, 1184.
12. Holmberg, K.; Matthews, A. Coatings Tribology, 2nd ed.; Elsevier: Amsterdam, 2009.
13. Holmberg, K.; Ronkainen, H.; Laukkanen, A.; Wallin, K.; Erdemir, A.; Eryilmaz, A. Wear 2008, 264, 877.
14. Holmberg, K.; Ronkainen, H.; Laukkanen, A.; Wallin, K. Surf Coat Technol 2007, 202, 1034.
15. Holmberg, K.; Laukkanen, A.; Ronkainen, H.; Wallin, K.; Varjus, S.; Koskinen, J. Surf Coat Technol 2006, 200, 3793.
16. Holmberg, K.; Laukkanen, A.; Ronkainen, H.; Wallin, K.; Varjus, S.; Koskinen, J. Surf Coat Technol 2006, 200, 3810.
17. Holmberg, K.; Laukkanen, A.; Ronkainen, H.; Wallin, K.; Varjus, S.; Koskinen, J. Surf Coat Technol 2006, 200, 3824.
18. Laugier, M. Thin Solid Films 1981, 76, 289.
19. Burnett, P.J.; Rickerby, D. S. Thin Solid Films 1987, 154, 403.
20. Laugier, M. T. Thin Solid Films 1984, 117, 243.
21. Burnett, P. J.; Rickerby, D. S. Thin Solid Films 1988, 157, 233.
22. Bull, S. J.; Rickerby, D. S.; Matthews, A.; Legland, A.; Pau, A. R.; Valli, J. Surf Coat Technol 1988, 36, 503.
23. Schwarzer, N. J Mater Res 2009, 24, 1032.
24. Schwarzer, N. Int J Surf Sci Eng 2007, 1, 239.
25. Oliver, W. C.; Pharr, G. M. J Mater Res 1992, 7, 1564.
26. Chudoba, T.; Herrmann, K. Härtereitechnische Mitteilungen HTM 2001, 56, 258.
27. Bolshakov, A.; Oliver, W. C.; Pharr, G. M. MRS Symp Proc 1995, 356, 675.
28. Pharr, G. M.; Bolshakov, B. J Mater Res 2002, 17, 2260.
29. Oliver, W. C.; Pharr, G. M. J Mater Res 2004, 19, 3.
30. Schwarzer, N. J Phys D: Appl Phys 2004, 37, 2761.
31. Schwarzer, N. ASME J Tribol 2000, 122, 672.
32. Chudoba, T.; Schwarzer, N.; Richter, F. Surf Coat Technol 2002, 154, 140.
33. Linss, V.; Hermann, I.; Schwarzer, N.; Kreissig, U.; Richter, F. Surf Coat Technol 2003, 163–164, 220.
34. Schwarzer, N. Habilitationsschrift der TU-Chemnitz 2004, FB Physik Fester Körper, http://archiv.tu-chemnitz.de/pub/2004/0077.
35. Linss, V.; Schwarzer, N.; Chudoba, T.; Karniychuk, M.; Richter, F. Surf Coat Technol 2005, 195, 287.
36. Chudoba, T.; Schwarzer, N.; Linss, V.; Richter, F. Thin Solid Films 2004, 469–470, 239.
37. Schwarzer, N.; Chudoba, T.; Pharr, G. M. Surf Coat Technol 2006, 200, 4220.
38. Chudoba, T.; Griepentrog, M.; Dück, A.; Schneider, D.; Richter, F. J Mater Res 2004, 19, 301.
39. Schwarzer, N.; Chudoba, T.; Richter, F. Surf Coat Technol 2006, 200, 5566.
40. Schwarzer, N. Thin Solid Films 2006, 494, 168.
41. Puschmann, R.; Schwarzer, N.; Richter, F.; Frühauf, S.; Schulz, S. E. Z. Metallkd 2005, 96, 1.
42. Herrmann, M.; Schwarzer, N.; Richter, F.; Frühauf, S.; Schulz, S. E. Surf Coat Technol 2006, 201, 4305.

43. Akhtar, R.; Sherratt, M. J.; Bierwisch, N.; Derby, B.; Mummery, P. M.; Watson, R. E. B.; Schwarzer, N. Mater Res Soc Proc 2008, 1097, GG01.
44. Akhtar, R.; Schwarzer, N.; Sherratt, M. J.; Watson, R. E. B.; Graham, H. K.; Trafford, A. W.; Mummery, P. M.; Derby, B. J Mater Res 2009, 24, 638.
45. Schwarzer, N.; Pharr, G. M. Thin Solid Films 2004, 469–470, 194.
46. FilmDoctor: Software package for the modelling of contact and internal load problems of porous, layered and nanostructured materials, available at www.siomec.de/FilmDoctor
47. ISA: Indentation-Scratch-Analyzer, Software package for the analysis of contact experiments, especially indentation and scratch tests, for arbitrarily layered materials www.siomec.de/ISA
48. Schwarzer, N.; Hermann, I.; Chudoba, T.; Richter, F. Surf Coat Technol 2001, 146–147, 371.